HHS Public Access

Author manuscript

Cancer. Author manuscript; available in PMC 2024 March 27.

Published in final edited form as:

Cancer. 2023 June 01; 129(11): 1744–1751. doi:10.1002/cncr.34704.

Bone marrow niche chemoprotection of metastatic solid tumors mediated by CYP3A4

Gabriel Ghiaur, MD, PhD,

Kenneth C. Valkenburg, PhD,

Christopher Esteb, BSc,

Alexander Ambinder, MD,

Philip H. Imus, MD,

Kenneth J. Pienta, MD,

Richard J. Jones, MD

Sidney Kimmel Comprehensive Cancer Center, Johns Hopkins University, Baltimore, Maryland, USA

Abstract

Background: The bone/bone marrow is one of the most common sites for metastatic solid tumors. Moreover, the tumor microenvironment is an essential part of cancer homeostasis. Previously, it was shown that cytochrome P450 enzymes (CYPs) are present in the bone marrow (BM) microenvironment, particularly in the mesenchymal stroma cells, at levels comparable to those of hepatocytes. It was found that the CYPs play important roles in nurturing and maintaining normal hematopoietic stem cells as well as multiple myeloma and leukemia cells, including protecting them from toxic insults. It was hypothesized that the CYPs in the BM microenvironment might play a similar role in solid tumors metastatic to bone.

Methods: The interaction between the BM microenvironment and malignant cells that routinely metastasize to the bone (lung, breast, and prostate cancer) was modeled. Via genetic engineering and pharmacological approaches, the role of stromal cytochrome P450 3A4 (CYP3A4) in drug resistance promoted by the BM microenvironment in niche–cancer models in vitro and in vivo was interrogated.

Results: BM stroma protected prostate, breast, and lung cancer cells from cytotoxic chemotherapy. Stromal CYP3A4 was at least partially responsible for this protection in vitro

Correspondence: Gabriel Ghiaur, Bunting-Blaustein Cancer Research Building, 1650 Orleans St, Rm 243, Baltimore, MD 21287, USA. gghiaur1@jhmi.edu.

AUTHOR CONTRIBUTIONS

Gabriel Ghiaur: Experiment design, analysis, and writing–original draft. **Kenneth C. Valkenburg:** Experimentation, analysis, and writing–original draft. **Christopher Esteb:** Experimentation. **Alexander Ambinder:** Analysis and writing–original draft. **Philip H. Imus:** Analysis. **Kenneth J. Pienta:** Project design and writing–review and editing. **Richard J. Jones:** Project design and writing–review and editing.

CONFLICT OF INTEREST STATEMENT

Kenneth J. Pienta is a consultant for Cue Biopharma. The other authors declare no conflicts of interest.

and in vivo. Moreover, inhibiting CYP3A4 with clarithromycin overcame the stroma-mediated chemoresistance toward prostate, breast, and lung cancer cells.

Conclusions: These results suggest that, similar to observations from hematologic malignancies, the BM microenvironment, through expression of CYPs, creates a sanctuary site from chemotherapy for metastatic solid tumors. Targeting these sanctuaries holds promise for eradicating bone metastasis in solid tumors.

Keywords

bone marrow microenvironment; cancer stem cells; cytochrome P450 3A4 (CYP3A4); drug resistance; metastatic disease; prostate cancer

INTRODUCTION

Most cancer-related deaths result from metastasis; the bone/bone marrow is one of the most common sites for metastatic solid tumors, especially in prostate, breast, and lung cancer.[1] The majority of men with prostate cancer and women with breast cancer have bone metastases when they die of their disease.[2] Understanding the cellular and molecular events that contribute to the metastatic process remains an important work in progress.

The tumor microenvironment is an essential part of cancer homeostasis. Bidirectional interactions between malignant cells and their surrounding stroma contribute to multiple aspects of cancer biology ranging from carcinogenesis to resistance to therapy.[3] Previously, we showed that cytochrome P450 enzymes (CYPs) are present in the bone marrow (BM) microenvironment, particularly in the mesenchymal stroma cells (MSCs), at levels comparable to those of hepatocytes.[4] Moreover, we found that CYPs in the BM stem cell niche play critical roles in nurturing and maintaining normal hematopoietic stem cells (HSCs).[5] Our data further suggest that CYPs within the BM microenvironment play critical roles in multiple myeloma and leukemia homeostasis, including protecting the cancer cells from cytotoxic chemotherapy.[4,6,7]

We hypothesized that, similar to hematologic malignancies, solid tumors metastatic to bone would likely be protected by CYPs in the BM microenvironment. Here we show, using a combination of in vivo and in vitro coculture models of prostate, breast, and lung cancer, that human BM stroma can in fact protect these solid tumors from chemotherapy. Moreover, this chemoresistance can be overcome by clinically applicable cytochrome P450 3A4 (CYP3A4) inhibitors.

MATERIALS AND METHODS

Cell lines and primary BM MSCs

Cell lines—The human fetal BM MSC line F/STRO was a kind gift from Dr Pierre Marie[8] and was cultured in Dulbecco's modified Eagle's medium (Gibco, Rockville, Maryland) with 10% fetal calf serum (FCS; Sigma-Aldrich), 100 μg/mL penicillin–streptomycin (P/S; Gibco), and 2 mM L-glutamine (Life Technologies). The human prostate cancer cell lines PC3[9] and C4-2B,[10] the human breast cancer cell line MCF7[11] (American Type Culture

Collection), and the human lung cancer cell line PC9[12] (Millipore-Sigma) were cultured in Roswell Park Memorial Institute 1640 (Gibco) with 10% FCS, 100 μg/mL P/S (Gibco), and 2 mM L-glutamine (Life Technologies). For adherent cell removal, media were removed, and the flasks were washed with phosphate-buffered saline (Gibco) twice; 0.25% trypsin (Gibco) was added for 60 s at 37°C, and the cells were then diluted with media and centrifuged to remove the trypsin.

Primary human BM MSCs—Primary human BM MSCs were derived from the plastic-adherent fraction of mononuclear BM cells as we have previously published.[4,6,7,13] Briefly, BM aspirates were cultured in the presence of Iscove's modified Dulbecco's medium (Gibco) supplemented with 5% horse serum (Gibco), 15% FCS, 10^{-5} M hydrocortisone 21hemisuccinate (Sigma-Aldrich), 100 μg/mL P/S, and 10^{-4} M β-mercaptoethanol (Sigma-Aldrich) at 33°C. Subconfluent cultures were subsequently passaged using dissociation with trypsin as described above. The passage number of primary BM MSCs was recorded.

All normal donors provided informed consent under a Johns Hopkins Medicine Institutional Review Board–approved protocol according to the Declaration of Helsinki.

In vitro drug treatment—To determine the half-maximal inhibitory concentration (IC_{50}), individual cancer cells were cultured on six-well plates and treated with increasing concentrations of docetaxel (Selleck Chemical LLC, Houston, Texas) in the presence or absence of 10^{-6} M clarithromycin (Sigma), an irreversible CYP3A4 inhibitor. Live cells were counted using 0.4% trypan blue (Gibco) after 72 h. For coculture experiments, F/STRO stroma cells expressing green fluorescent protein (GFP; see below) or those transduced with CYP3A4-targeting short hairpin RNA (shRNA) (see below) were irradiated (20 Gy) to prevent overgrowth and mixed 1:1 with cancer cells. The cocultures were plated on six-well plates and treated with increasing concentrations of docetaxel. After 72 h, the cocultures were trypsinized, live cells were counted using 0.4% trypan blue, and the percentage of F/STRO cells (GFP-positive) and cancer cells (GFP-negative) was determined by flow cytometry.

Lentiviral infections

CYP3A4 knockdown by shRNA—As previously published,[4,6] lentiviral vectors expressing CYP3A4-targeting shRNA (The RNAi Consortium, Broad Institute, Cambridge, Massachusetts) and the empty lentiviral vector pGIPZ (Open Biosystems, Lafayette, Colorado) were transfected together with pCMV-dR8.9– and VSV-G–expressing plasmids into 293T cells using Lipofectamine 2000 (Invitrogen, Carlsbad, California) for lentiviral supernatant production. F/STRO cells or primary human BM MSCs at Passage 2 were incubated with the viral supernatant and 8 μg/mL Polybrene (Sigma-Aldrich) for transduction. After at least 48 h, the cells were treated with 8 μg/mL puromycin (Sigma-Aldrich) to select for positive clones. The CYP3A4 gene expression level of the infected cells was confirmed by quantitative reverse transcriptase–polymerase chain reaction. F/STRO cells infected with pGIPZ control expressed GFP and were used for the coculture conditions described above. Primary BM MSCs at Passage 5 infected with either shRNA or pGIPZ control were used for stroma–prostate cancer xenograft models as described below.

Luciferase—To mark the PC3 cells with luciferase, pLenti-CMV-LUC-Puro lentiviral vectors (plasmid 17477; Addgene, Cambridge, Massachusetts) were used to generate lentiviral supernatants as we have previously published,[4,6,8] and the PC3 cells were incubated with the lentiviral supernatant in the presence of 8 μg/mL Polybrene (Sigma). After 48 h, the transduced cells were selected using puromycin (Gibco).

Mouse xenograft models of prostate cancer

Two mouse xenograft models were developed.

A disseminated model of prostate cancer was created using intracardiac injection of luciferase-labeled PC3 cells (PC3-Luc) as previously published.[14] Briefly, subconfluent PC3-Luc cells were trypsinized the day of the injections, washed, and suspended in sterile phosphate-buffered saline (Gibco). Non obese diabetes severe combined immunodeficient and interleukemia 2 receptor gamma knockout [NOD SCID IL-2γ−/− (NSG) mice (The Jackson Laboratory, Bar Harbor, Maine) were anesthetized with 2.5% inhaled isoflurane (VetOne, Boise, Idaho) and, 200,000 cells in a 100-μL volume were injected into the left ventricle of the heart using a 0.5-mL insulin syringe with a 29½-gauge needle. One week after injection, the mice were imaged for the presence of bioluminescence using the In Vivo Imaging System (IVIS; PerkinElmer, Alameda, California). For imaging, the mice were exposed to 30 mg/kg D-luciferin (Xenogen) via intraperitoneal injection 10–15 min prior to imaging and anesthetized using isoflurane (VetOne). The images were analyzed with Living Image software 2.5 (PerkinElmer) and the data were quantified as photons/s. Mice that showed significant lung signals were excluded. The rest of the mice were randomly assigned to four treatment groups: vehicle control, clarithromycin only, docetaxel only, and clarithromycin plus docetaxel. Clarithromycin (Sigma) was given intraperitoneally at 20 mg/kg twice per week on consecutive days. Docetaxel (Armas Pharmaceuticals, Inc, Manalapan, New Jersey) was given intraperitoneally at 20 mg/kg once per week on the second day of clarithromycin treatment. Vehicle was given intraperitoneally to control mice on the same days that clarithromycin was administered. Tumor burden was assessed weekly by bioluminescence imaging (BLI) using IVIS.

A stroma–prostate cancer xenograft model was developed as we previously published for leukemia and multiple myeloma.[4,6,13] Briefly, 100,000 PC3-Luc cells were mixed with 100,000 primary human BM stroma cells infected with either control lentivirus (control stroma) or anti-CYP3A4 shRNA lentivirus (CYP3A4 knockdown [KD] stroma). The stroma plus prostate cancer cells were injected into each flank (control stroma in the right flank; CYP3A4 KD stroma in the left flank) of 16-week-old NSG mice. After tumor engraftment, the mice were treated with docetaxel at 20 mg/kg/week by IP injection. The tumor burden was assessed weekly by BLI. Liver metastasis was assessed via BLI and visual confirmation of the liver upon sacrifice. After whole-body imaging, IVIS software was used to analyze a selected region of interest overlapping the liver, and the same region of interest was used to establish the signal for each mouse for direct comparison. Visible liver metastases were quantified during necropsy. For assessment of bone metastasis, leg bones (femurs, tibiae, and fibulae) were removed from the sacrificed mice and x-rayed on a Faxitron instrument

(Faxitron, Tucson, Arizona). Metastatic lesions were visualized upon x-ray analysis as indicated by the loss of bone tissue.

Statistical analysis—For in vitro experiments, statistical analysis was performed by using a two-tailed unpaired Student *t*-test to compare the averages of groups and calculate the *p* value. For in vivo experiments, on the basis of preliminary data from our laboratory, we assumed a standard deviation of 0.5 μ, where μ is the mean luminescence in each group. We considered a 1-log reduction in luminescence to be biologically significant. Using these assumptions, we calculated that five tumors are needed in each arm to achieve an α value of 0.05 and a power of 0.80.

RESULTS

BM stroma protects prostate cancer cells from chemotherapy in vitro

Docetaxel is now the standard of care for patients with metastatic hormone-responsive prostate cancer based on several large prospective randomized trials.[15,16] In coculture models, both PC3 and C4-2B prostate cancer cells were protected from docetaxel-induced kill by BM stroma (Figure 1A,B). Stroma increased docetaxel's IC_{50} against the prostate carcinoma PC3 cells by 10-fold (IC_{50}, 46 nM for stroma coculture vs. 3.8 nM for stroma-free; $p < .01$; Figure 1C,D). Docetaxel is cleared from the circulation mostly via hepatic CYP3A4-mediated inactivation.[17] We have previously shown that BM stroma cells express CYP3A4 at levels comparable to those of hepatocytes.[4] To test whether BM stroma cell expression of CYP3A4 contributes to the observed protection from docetaxel, we have generated F/STRO BM stroma cells deficient in CYP3A4 via a lentiviral vector–mediated shRNA KD against CYP3A4 (KD-F/STRO). KD-F/STRO had no protective effect against the docetaxel-mediated kill of PC3 cells (Figure 1A) or C4-2B cells (Figure 1B). Concomitant treatment with the CYP3A4 inhibitor clarithromycin rescued both the PC3 and C4–2B cell sensitivity to docetaxel in coculture conditions with wild-type (WT) stroma (Figure 1). Clarithromycin had no effect in stroma-free cultures (Figure 1C,D); this supports the cell-extrinsic role of CYP3A4 in these coculture systems.

BM stroma similarly protects breast and lung cancers from chemotherapy in vitro

Next, we tested whether similar stroma-dependent drug inactivation protects other solid tumor cells metastatic to bone. For this purpose, we used adenocarcinoma cell lines representative of breast and lung cancers, two tumors that can commonly present with bone metastasis. We tested their sensitivity to doxorubicin, a clinically active chemotherapeutic agent used in both tumor types.[18,19] As with prostate cancer, stroma protected both MCF7 breast cancer cells and PC9 lung cancer cells, and this effect was eliminated by CYP3A4 KD and overcome by clarithromycin (Figure 2).

BM stroma protects prostate cancer from chemotherapy in vivo

To investigate the potential impact of stromal CYP3A4 inhibition on chemotherapy activity in vivo, we tested the stroma–cancer interaction in a complex subcutaneous xenograft model. For this, we derived human primary BM stroma cells from healthy volunteers and transduced them with a lentiviral vector expressing shRNA targeting CYP3A4 (KD stroma)

or control lentiviral vector (WT stroma). Early-passage KD or WT stroma was mixed with PC3 prostate cancer cells expressing luciferase (PC3-Luc) and inoculated subcutaneously in the left and respectively right flank of NSG mice. After tumor engraftment was documented via BLI, the mice were treated with docetaxel and the tumor burden was measured by BLI. Similar to the in vitro models, after 13 weeks of treatment, tumors that contained KD stroma had a significantly lower tumor burden compared to WT stroma–containing tumors (Figure 3; $p < .05$).

To test whether stromal CYP3A4 contributes to the resistance of prostate cancer cells to docetaxel, we used a systemic, metastatic xenograft model in which PC3-Luc cells were delivered via intracardiac injection. After injection, the mice were randomly assigned to one of four treatment groups (dimethyl sulfoxide [DMSO], clarithromycin, docetaxel, or docetaxel plus clarithromycin), and their tumor burden was monitored weekly by measuring total bioluminescence. Whereas animals treated with DMSO or clarithromycin showed a steady increase in tumor burden and succumbed to the disease by Week 5, treatment with docetaxel for 9 weeks prevented tumor growth but did not eradicate the tumor (Figure 4A). Addition of clarithromycin to docetaxel decreased the bioluminescence below the background control levels (Figure 4A). To test whether the tumor was indeed eliminated in these mice, the treatment was stopped after 9 weeks. Mice treated with docetaxel alone died by Week 13. The tumor remained below background levels in the docetaxel plus clarithromycin group up until sacrifice at 17 weeks.

Postmortem macroscopic and radiologic analysis demonstrated that the mice in the DMSO and clarithromycin groups had widespread metastases in the liver (Figure 4B) and bone (Figure 4C). Although no detectable liver metastases were present in the docetaxel-alone group (Figure 4B), mice from this group had clear bone metastases in the spine and legs (Figure 4C) upon succumbing to metastatic PC3 prostate cancer. The addition of clarithromycin to docetaxel, however, eliminated not only liver metastasis but also bone metastasis and kept the animal tumor-free even after the treatment was stopped. These data suggest that, similar to our in vitro coculture model, BM stroma inhibits the ability of docetaxel to eliminate metastatic cells spread to the bone. Even more so, although clarithromycin undoubtedly affected the systemic pharmacokinetics of docetaxel, it was also able to reverse the protective ability of the BM stroma.

DISCUSSION

Metastatic disease is the cause of most of the morbidity and mortality related to cancer. The spectrum of organs affected by metastases depends on the specific type of cancer, with bone/bone marrow the number one site for breast and prostate cancer as well as a common site for lung cancer. The sites of metastases are undoubtedly a function of many variables. Beyond the passive role of circulation patterns (e.g., liver for gastrointestinal malignancy spread), metastatic cell dissemination is actively influenced by both intrinsic and extrinsic cancer cell mechanisms.[20]

The presence of a supportive microenvironment is clearly one of the mechanisms important for cancer cell dissemination.[20] The BM niche represents an example of such a highly

complex microenvironment that ensures the survival, self-renewal, and differentiation of HSCs.[21] Although the exact mechanisms by which the BM microenvironment supports metastatic tumor homing and growth are still under investigation, the same mechanisms that enhance HSC properties may also be of particular benefit to cancer cells.[22] Drug-metabolizing enzymes appear to represent a biochemical barrier between the plasma and the BM microenvironment, resulting in a sanctuary site from drugs. In particular, CYPs in the BM microenvironment appear to maintain and protect both normal hematopoietic progenitor cells[5] and hematologic malignancies.[4,6,7,23,24] Here, our data suggest that the BM microenvironment is similarly supportive of solid tumors that seed these niches. In our mouse model of metastatic prostate cancer, docetaxel was able to eliminate hepatic but not bone metastases. However, the addition of the CYP3A4 inhibitor clarithromycin to docetaxel was able to also eliminate the bone metastases that remained after docetaxel alone, and this suggests an effect on local CYP3A4 activity.

Pharmacokinetic parameters such as affinity and velocity constants may allow CYPs to play different, but complementary, roles in the systemic (hepatic) and local (BM microenvironment) inactivation of drugs. CYP3A4 is highly expressed in the liver and intestines, likely as a way to provide systemic protection against toxic insults. In contrast, CYP3A4 in the BM microenvironment appears to provide local protection. Thus, CYP3A4 inhibition in the liver and intestines will be expected to lead to higher drug exposure systemically, with increased toxicity likely. Accordingly, CYP3A4 inhibition has been studied clinically, with the expected increased systemic drug levels and toxicity.[25–28] Pharmacologically adjusting cytotoxic chemotherapy doses to maintain safe systemic concentrations should lessen the systemic toxicity related to the inhibition of liver CYPs while removing barriers to therapeutic drug levels in the BM microenvironment.[4,6,7] A clinical trial to study this concept by combining clarithromycin with docetaxel in docetaxel- or cabazitaxel-resistant metastatic castration-resistant prostate cancer has been developed (NCT03043989).

ACKNOWLEDGMENTS

This work was supported in part by National Institutes of Health Grants P01 CA15396, P01 CA225618, P30 CA006973, and LLS TRP 6473-15.

REFERENCES

1. Mundy GR. Metastasis to bone: causes, consequences and therapeutic opportunities. Nat Rev Cancer. 2002;2(8):584–593. doi:10.1038/nrc867 [PubMed: 12154351]
2. Coleman RE. Metastatic bone disease: clinical features, pathophysiology and treatment strategies. Cancer Treat Rev. 2001;27(3):165–176. doi:10.1053/ctrv.2000.0210 [PubMed: 11417967]
3. Ghiaur G, Wroblewski M, Loges S. Acute myelogenous leukemia and its microenvironment: a molecular conversation. Semin Hematol. 2015;52(3):200–206. doi:10.1053/j.seminhematol.2015.03.003 [PubMed: 26111467]
4. Alonso S, Su M, Jones JW, et al. Human bone marrow niche chemoprotection mediated by cytochrome P450 enzymes. Oncotarget. 2015;6(17):14905–14912. doi:10.18632/oncotarget.3614 [PubMed: 25915157]
5. Ghiaur G, Yegnasubramanian S, Perkins B, Gucwa JL, Gerber JM, Jones RJ. Regulation of human hematopoietic stem cell self-renewal by the microenvironment's control of retinoic acid signaling.

Proc Natl Acad Sci USA. 2013;110(40):16121–16126. doi:10.1073/pnas.1305937110 [PubMed: 24043786]

6. Chang YT, Hernandez D, Alonso S, et al. Role of CYP3A4 in bone marrow microenvironment-mediated protection of FLT3/ITD AML from tyrosine kinase inhibitors. Blood Adv. 2019;3(6):908–916. doi:10.1182/bloodadvances.2018022921 [PubMed: 30898762]
7. Su M, Alonso S, Jones JW, et al. All-trans retinoic acid activity in acute myeloid leukemia: role of cytochrome P450 enzyme expression by the microenvironment. PLoS One. 2015;10(6):e0127790. doi:10.1371/journal.pone.0127790 [PubMed: 26047326]
8. Ahdjoudj S, Lasmoles F, Oyajobi BO, Lomri A, Delannoy P, Marie PJ. Reciprocal control of osteoblast/chondroblast and osteoblast/adipocyte differentiation of multipotential clonal human marrow stromal F/STRO-1(+) cells. J Cell Biochem. 2001;81(1):23–38. doi:10.1002/1097-4644(20010401)81:1<23::aid-jcb1021>3.0.co;2-h [PubMed: 11180395]
9. Kaighn ME, Narayan KS, Ohnuki Y, Lechner JF, Jones LW. Establishment and characterization of a human prostatic carcinoma cell line (PC-3). Invest Urol. 1979;17(1):16–23. [PubMed: 447482]
10. Thalmann GN, Anezinis PE, Chang SM, et al. Androgen-independent cancer progression and bone metastasis in the LNCaP model of human prostate cancer. Cancer Res. 1994;54(10):2577–2581. [PubMed: 8168083]
11. Sugarman BJ, Aggarwal BB, Hass PE, Figari IS, Palladino MA Jr, Shepard HM. Recombinant human tumor necrosis factor-alpha: effects on proliferation of normal and transformed cells in vitro. Science. 1985;230(4728):943–945. doi:10.1126/science.3933111 [PubMed: 3933111]
12. Lee YC, Saijo N, Sasaki Y, et al. Clonogenic patterns of human pulmonary adenocarcinoma cell lines (PC-9, PC-13 and PC-14) and how they influence the results of test for chemosensitivity to cisplatin in the human tumor clonogenic assay. Jpn J Clin Oncol. 1985;15(4): 637–644. [PubMed: 4094096]
13. Alonso S, Hernandez D, Chang YT, et al. Hedgehog and retinoid signaling alters multiple myeloma microenvironment and generates bortezomib resistance. J Clin Investig. 2016;126(12):4460–4468. doi:10.1172/JCI88152 [PubMed: 27775549]
14. Axelrod HD, Valkenburg KC, Amend SR, et al. AXL is a putative tumor suppressor and dormancy regulator in prostate cancer. Mol Cancer Res. 2019;17(2):356–369. doi:10.1158/1541-7786.MCR-18-0718 [PubMed: 30291220]
15. James ND, Sydes MR, Clarke NW, et al. Addition of docetaxel, zoledronic acid, or both to first-line long-term hormone therapy in prostate cancer (STAMPEDE): survival results from an adaptive, multiarm, multistage, platform randomised controlled trial. Lancet. 2016;387(10024):1163–1177. doi:10.1016/S0140-6736(15)01037-5 [PubMed: 26719232]
16. Sweeney CJ, Chen YH, Carducci M, et al. Chemohormonal therapy in metastatic hormone-sensitive prostate cancer. N Engl J Med. 2015;373(8):737–746. doi:10.1056/NEJMoa1503747 [PubMed: 26244877]
17. Clarke SJ, Rivory LP. Clinical pharmacokinetics of docetaxel. Clin Pharmacokinet. 1999;36(2):99–114. doi:10.2165/00003088-199936020-00002 [PubMed: 10092957]
18. Nabholtz JM, Mackey JR, Smylie M, et al. Phase II study of docetaxel, doxorubicin, and cyclophosphamide as first-line chemotherapy for metastatic breast cancer. J Clin Oncol. 2001;19(2):314–321. doi:10.1200/JCO.2001.19.2.314 [PubMed: 11208821]
19. Spiro SG, James LE, Rudd RM, et al. Early compared with late radiotherapy in combined modality treatment for limited disease small-cell lung cancer: a London Lung Cancer Group multicenter randomized clinical trial and meta-analysis. J Clin Oncol. 2006;24(24):3823–3830. doi:10.1200/JCO.2005.05.3181 [PubMed: 16921033]
20. Oskarsson T, Batlle E, Massague J. Metastatic stem cells: sources, niches, and vital pathways. Cell Stem Cell. 2014;14(3):306–321. doi:10.1016/j.stem.2014.02.002 [PubMed: 24607405]
21. Raaijmakers MH, Scadden DT. Divided within: heterogeneity within adult stem cell pools. Cell. 2008;135(6):1006–1008. doi:10.1016/j.cell.2008.11.034 [PubMed: 19070570]
22. Shiozawa Y, Pedersen EA, Havens AM, et al. Human prostate cancer metastases target the hematopoietic stem cell niche to establish footholds in mouse bone marrow. J Clin Investig. 2011;121(4): 1298–1312. doi:10.1172/JCI43414 [PubMed: 21436587]

23. Alonso S, Jones RJ, Ghiaur G. Retinoic acid, CYP26, and drug resistance in the stem cell niche. Exp Hematol Oncol. 2017;54:17–25. doi:10.1016/j.exphem.2017.07.004

24. Su M, Chang YT, Hernandez D, Jones RJ, Ghiaur G. Regulation of drug metabolizing enzymes in the leukaemic bone marrow microenvironment. J Cell Mol Med. 2019;23(6):4111–4117. doi:10.1111/jcmm.14298 [PubMed: 30920135]

25. Engels FK, Ten Tije AJ, Baker SD, et al. Effect of cytochrome P450 3A4 inhibition on the pharmacokinetics of docetaxel. Clin Pharmacol Ther. 2004;75(5):448–454. doi:10.1016/j.clpt.2004.01.001 [PubMed: 15116057]

26. Tanaka C, Yin OQ, Smith T, et al. Effects of rifampin and ketoconazole on the pharmacokinetics of nilotinib in healthy participants. J Clin Pharmacol. 2011;51(1):75–83. doi:10.1177/0091270010367428 [PubMed: 20702754]

27. Van Veldhuizen PJ, Reed G, Aggarwal A, Baranda J, Zulfiqar M, Williamson S. Docetaxel and ketoconazole in advanced hormone-refractory prostate carcinoma: a phase I and pharmacokinetic study. Cancer. 2003;98(9):1855–1862. doi:10.1002/cncr.11733 [PubMed: 14584067]

28. Venkatakrishnan K, Rader M, Ramanathan RK, et al. Effect of the CYP3A inhibitor ketoconazole on the pharmacokinetics and pharmacodynamics of bortezomib in patients with advanced solid tumors: a prospective, multicenter, open-label, randomized, two-way crossover drug-drug interaction study. Clin Ther. 2009;31(pt 2):2444–2458. doi:10.1016/j.clinthera.2009.11.012 [PubMed: 20110052]

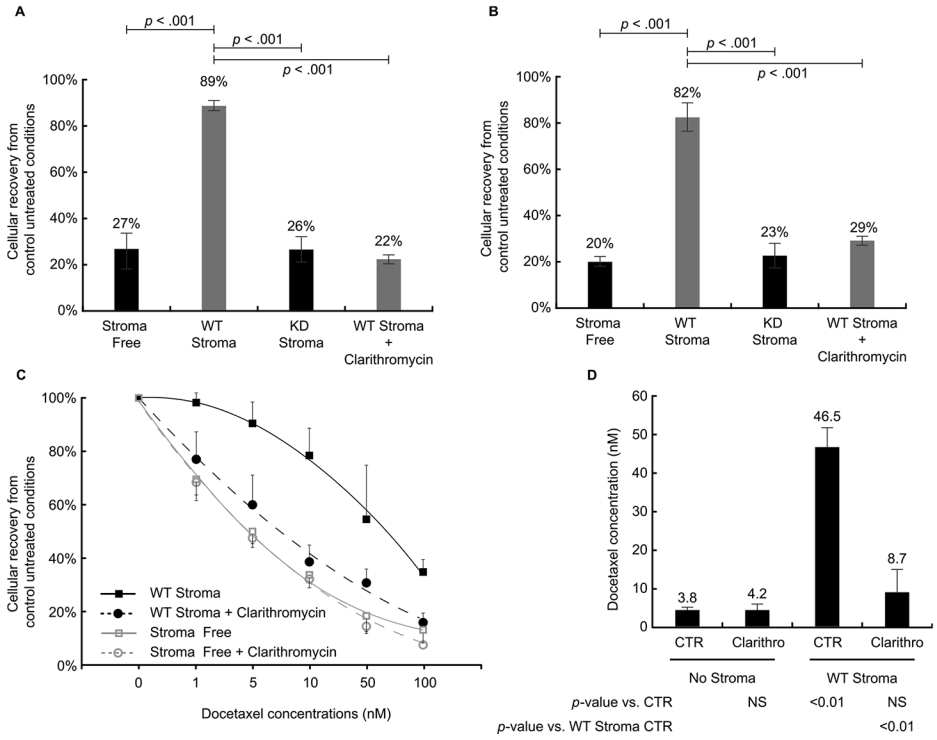

FIGURE 1.

Stromal CYP3A4 protects prostate cancer cells from docetaxel. (A) PC3 and (B) C4-2B prostate cancer cells were treated with docetaxel (5 nM) in the presence or absence of human BM–derived mesenchymal stroma cells (F/STRO WT stroma), shRNA-mediated knockdown of CYP3A4 (KD stroma), or clarithromycin. (C) Kill curve and (D) IC_{50} of docetaxel on PC3 cells. Data are presented as mean ± SD of three independent experiments; the *p* values depicted were obtained using an unpaired Student *t*-test. BM indicates bone marrow; CTR, control; CYP3A4, cytochrome P450 3A4; IC_{50}, half-maximal inhibitory concentration; KD, knockdown; NS, not significant; shRNA, short hairpin RNA; WT, wild-type.

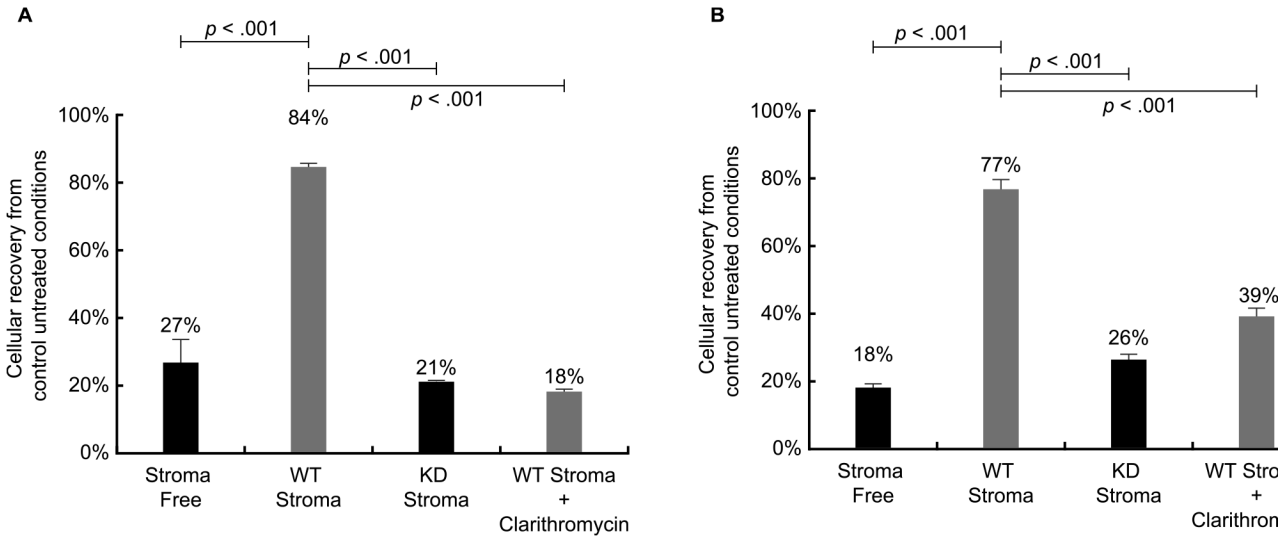

FIGURE 2.

Stromal CYP3A4 protects breast and lung cancer cells from doxorubicin. (A) MCF7 breast cancer cells and (B) PC9 lung cancer cells were treated with doxorubicin (0.5 μM) in the presence or absence of human BM–derived mesenchymal stroma cells (F/STRO WT stroma), shRNA-mediated knockdown of CYP3A4 (KD stroma), or clarithromycin. Data are presented as mean ± SD of three independent experiments; the *p* values depicted were obtained using an unpaired Student *t*-test. BM indicates bone marrow; CYP3A4, cytochrome P450 3A4; KD, knockdown; shRNA, short hairpin RNA; WT, wild-type.

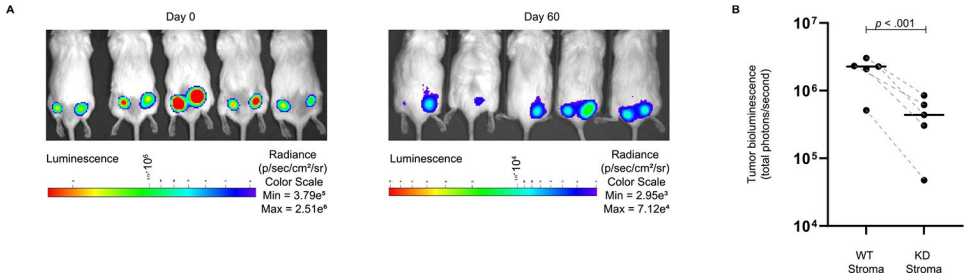

FIGURE 3.

Stromal CYP3A4 protects prostate cancer cells from docetaxel in vivo. (A) Bioluminescence activity at Days 0 and 60 in mice engrafted subcutaneously with PC3-luciferase mixed with either WT stroma (right flank) or shRNA targeting CYP3A4 (KD stroma; left flank) and treated with docetaxel at 20 mg/kg/week. One representative example of five independent experiments with similar results is shown. (B) Tumor burden was measured as photons/s. Dashed lines represent paired tumors found in individual mice. Horizontal lines represent the mean. The *p* values were obtained using an unpaired Student *t*-test. CYP3A4 indicates cytochrome P450 3A4; KD, knockdown; WT, wild-type.

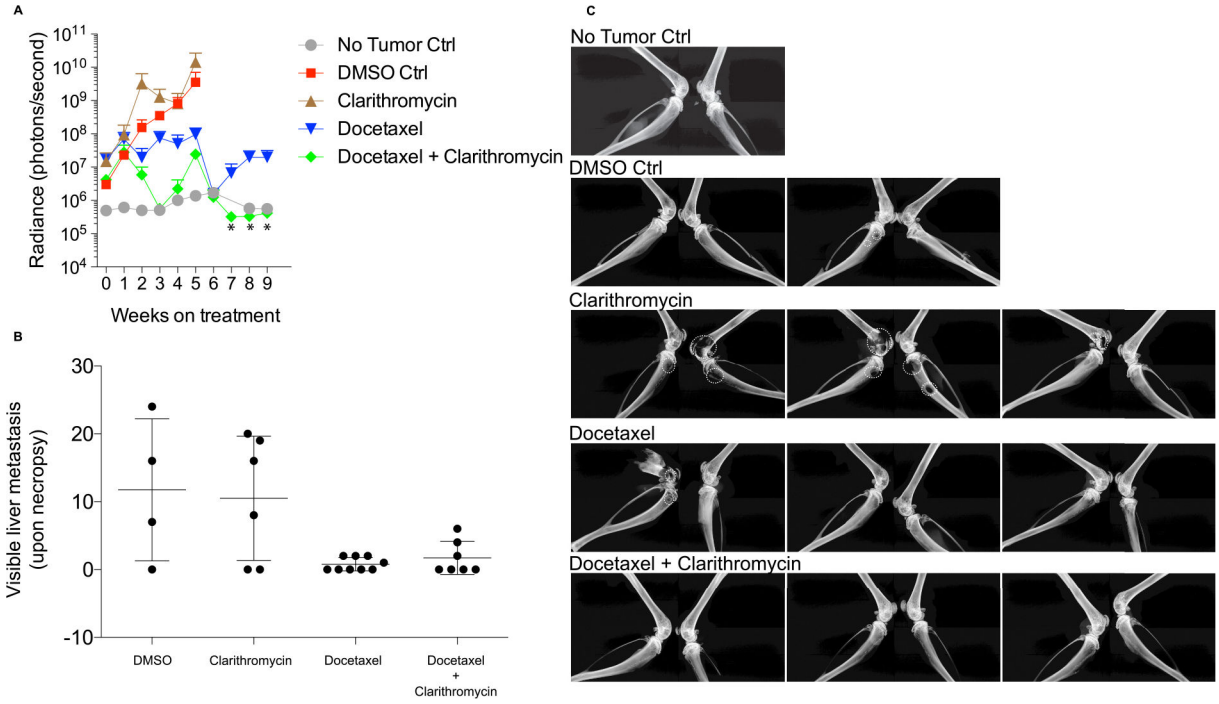

FIGURE 4.

Docetaxel controls systemic prostate cancer disease burden but does not sterilize the bone marrow. (A) Tumor burden in mice measured by total-body bioluminescence imaging after intracardiac injection of luciferase-labeled PC3 cells. Gray circles represent background bioluminescence from non–tumor-bearing mice. Data are presented as mean ± SD of three independent experiments with more than five mice per group. *$p < .01$ (docetaxel vs. docetaxel + clarithromycin) using an unpaired Student t-test. This analysis was conducted at Weeks 7, 8, and 9 of treatment. (B) The number of macroscopic liver metastases of individual mice at the time of necropsy. (C) Representative x-ray images of hind limbs of animals in Panels A and B at the time of death/sacrifice. The absence of bone matrix suggestive of bone metastasis is depicted with circles. Ctrl indicates control; DMSO, dimethyl sulfoxide.